

22. Applying an electric field of 0.2 V/Å in a nonself consistent calculation left the relative magnitudes of the DOS for  $C_{60}$  and  $C_{60} \cdot 2CHCl_3$  largely unchanged in the doping range from 2 to 3.5.
23. A. K. Bill, V. Z. Kresin, unpublished data.
24. T. Yildirim *et al.*, *Phys. Rev. Lett.* **77**, 167 (1996).
25. M. P. Gelfand, J. P. Lu, *Phys. Rev. Lett.* **68**, 1050 (1992).
26. O. Gunnarsson *et al.*, *Phys. Rev. Lett.* **74**, 1875 (1995).
27. M. Schluter, M. Lannoo, M. Needels, G. A. Baraff, D. Tomaneck, *J. Phys. Chem. Solids* **53**, 1473 (1992).
28. W. I. F. David *et al.*, *Nature* **353**, 147 (1991).
29. J. I. Langford, D. Louer, *Rep. Prog. Phys.* **59**, 131 (1996).
30. R. J. Hill, L. M. D. Cranswick, *J. Appl. Crystallogr.* **27**, 802 (1994).
31. O.G. thanks the Max-Planck-Forschungspreis, and R. D. thanks the Fonds der Chemischen Industrie (FCI)

for support. Research carried out in part at the National Synchrotron Light Source at Brookhaven National Laboratory, which is supported by the U.S. DOE, Division of Materials Sciences and Division of Chemical Sciences. The SUNY X3 beamline at NSLS is supported by the Division of Basic Energy Sciences of the U.S. DOE (grant no. DE-FG02-86ER45231).

26 November 2001; accepted 5 March 2002

# A High-Resolution Paleoclimate Record Spanning the Past 25,000 Years in Southern East Africa

Thomas C. Johnson,<sup>1\*</sup> Erik T. Brown,<sup>1</sup> James McManus,<sup>1</sup> Sylvia Barry,<sup>1†</sup> Philip Barker,<sup>2</sup> Françoise Gasse<sup>3</sup>

High-resolution profiles of the mass accumulation rate of biogenic silica and other geochemical proxies in two piston cores from northern Lake Malawi provide a climate signal for this part of tropical Africa spanning the past 25,000 years. The biogenic silica mass accumulation rate was low during the relatively dry late Pleistocene, when the river flux of silica to the lake was suppressed. Millennial-scale fluctuations, due to upwelling intensity, in the late Pleistocene climate of the Lake Malawi basin appear to have been closely linked to the Northern Hemisphere climate until 11 thousand years ago. Relatively cold conditions in the Northern Hemisphere coincided with more frequent north winds over the Malawi basin, perhaps resulting from a more southward migration of the Intertropical Convergence Zone.

Tropical Africa was cooler and drier during the last glacial maximum than it is today (1, 2). However, we have little information about higher frequency climate variability in the African tropics during the last glacial period or about the transition from ice age to interglacial conditions. Was there an abrupt shift to warm and wetter conditions? Was there monotonic evolution, or change by fits and starts? How does climate change in the African tropics relate to the signals registered in the ice sheets of Greenland and Antarctica? Some answers have been forthcoming from studies of lake sediments throughout much of Africa (1). But knowledge of the timing and nature of climate variability in much of tropical Africa still eludes us, as does an understand-

ing of its role in the global climate system.

Here, we present a high-resolution record of climate dynamics from two piston cores spanning the past 25,000 years in northern Lake Malawi (Fig. 1). We recovered six piston cores and seven multicores from the north basin of Lake Malawi in 1998 as part of an expedition of the International Decade for the East African Lakes (IDEAL) (3).

Two of the cores were selected for more detailed study: M98-1P (at 10°15.9'S, 34°19.1'E, and a 403-m depth) and M98-2P (at 9°58.6'S, 34°13.8'E, and a 363-m depth) (Fig. 1). Radiocarbon dates were obtained on organic matter at six horizons in M98-1P and at eight horizons in M98-2P, using accelera-

tor mass spectrometry (Table 1). Both cores show a distinct shift in sedimentation rates from about 0.2 mm per year before 12 thousand years ago (ka) to about 0.5 mm per year after that time. We sampled these cores at 1-cm intervals for biogenic silica analysis and at a lower resolution for other parameters, including incompatible trace metals, total and inorganic phosphorus, diatom concentration, and species assemblages.

The percent biogenic silica in the cores reflects the abundance of diatoms in the lake sediments. Other sources of biogenic silica (e.g., phytoliths and sponge spicules) are rare in comparison to diatoms. Diatoms dominate the phytoplankton in Lake Malawi throughout most of the year, especially during the dry windy season in austral winter, when primary production in the lake is at a maximum (4, 5). The percent biogenic silica was converted to a mass accumulation rate (BSi MAR) based on sediment porosity and density and the linear sedimentation rates.

The BSi MAR profiles of the two cores correlate well, and, at the millennial scale, show similarities to the Greenland ice core record (GRIP) of the oxygen isotope ratio ( $\delta^{18}O$ ) (Fig. 2). Both BSi MAR profiles show lower mean values in the Pleistocene sediments than in the Holocene deposits, and the transition from Pleistocene to Holocene values occurs in two abrupt steps, with an intervening interval of Pleistocene-like conditions. The timing of the glacial to interglacial transition, however, is different from the timing recorded in the GRIP record. The profiles exhibit an abrupt shift to higher values, beginning at about 13 ka, and then show a return to lower values about a thousand years later. The BSi MAR rises abruptly once again around 10.3 ka, to Holocene values. The initial rise to Holocene-like values at 13 ka

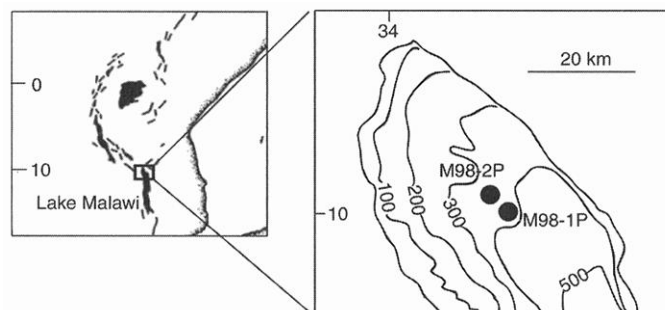


Fig. 1. Bathymetry of the north basin of Lake Malawi, showing the locations of the core sites. The contours are in meters.

<sup>1</sup>Large Lakes Observatory, University of Minnesota Duluth, Duluth, MN 55812, USA. <sup>2</sup>Department of Geography, Lancaster University, Lancaster LA1 4YB, UK. <sup>3</sup>Centre Européen de Recherche et d'Enseignement en Géosciences de l'Environnement, Centre National de la Recherche Scientifique, Université d'Aix-Marseille III, BP 80, 13545 Aix-en-Provence, Cedex 04, France.

\*To whom correspondence should be addressed. E-mail: tcj@umn.edu

†Present address: Harvard Forest, Post Office Box 68, Petersham, MA 01366, USA.

## REPORTS

occurred as the Northern Hemisphere plunged back into glacial-like conditions at the beginning of the Younger Dryas. Peaks and valleys of the Pleistocene portion of the BSi MAR profile are often antiphased with the GRIP record (Fig. 3). When BSi MAR values increase (i.e., toward Holocene values), the GRIP record shifts toward colder temperatures. The African tropical climate thus appears to have been linked to the ice sheet and climate dynamics of the Northern Hemisphere in the late Pleistocene. The Malawi BSi MAR record does not relate as closely to the Antarctic ice core records at Byrd or Vostok, nor to the tropical Atlantic sea surface temperature record (6), as it does to the Greenland records.

A geochemical mass balance of silica in the Lake Malawi system (7) demonstrates that a prolonged peak in the BSi MAR in the sediments, representing a few centuries or more, can only be supported by a change in the net input of dissolved silica to the lake or by shifting the location of diatom burial within the lake.

The first mechanism, a change in the silica supply, can explain the difference between glacial and interglacial BSi MARs. The low BSi MAR in Pleistocene sediments in the lake is attributed to a low river influx of silica during the relatively cool dry conditions that were pervasive throughout tropical Africa during the last glacial maximum (LGM) (1). The percentage of periphytic (benthic) diatoms in core M98-2P was unusually high, between 10 and 30%, from 23 to 15.7 ka, indicating a lowstand of Malawi at that time (Fig. 3) (8). The magnitude of this lowstand is not yet known, but was probably between 100 and 200 m lower than present, based on seismic reflection profiles and sediment core stratigraphy (9).

Other than possible ties at 22 and 16 ka, the Pleistocene lake level inferred from the diatom record does not appear to be tightly coupled to millennial-scale fluctuations in BSi MAR within the Pleistocene. Thus, we turn to a second mechanism to explain millennial-scale variability, a relative (not absolute) shift in diatom productivity and burial from the south to the north basin of the lake. We hypothesize that this mechanism is caused by more frequent or stronger winds out of the north that would promote upwelling in the north basin.

Wind transport of volcanic ash from the north supports this hypothesis. Volcanic ash layers in northern Lake Malawi sediments are enriched in certain incompatible elements (i.e., resistant to incorporation into mineral phases, thus enriched in volcanic glass), including niobium (10). Consequently, the relative abundance of volcanically derived material in the sediments is

reflected in a profile of Nb/Ti. The intervals of relatively high BSi MAR before 11 ka all coincide with times of relatively high Nb/Ti ratios (Fig. 3) (11).

The volcanic ash in Lake Malawi is de-

rived from just one area, the Rungwe volcanoes to the north of the lake (Fig. 1). These are late Tertiary to Holocene (as recent as the early 19th century) basalts and phonolytic trachytes (12). Two discrete ash layers de-

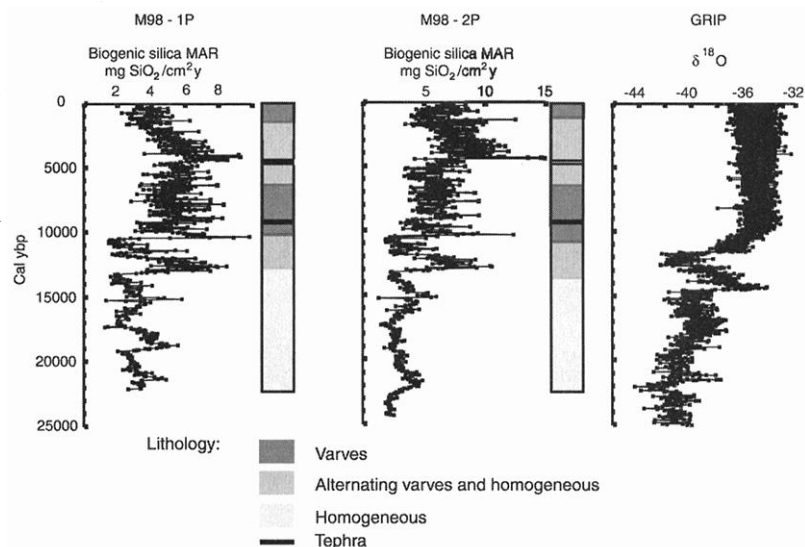


**Fig. 2.** BSi MARs and lithology (3) in cores M98-1P and M98-2P (left and center) and the GRIP δ<sup>18</sup>O record (right). The analytical procedure for biogenic silica was modified to entail a single determination of dissolved silica in the digestion solution (0.5 M NaOH at 85°C) after the sediment digested for 42.5 min. The timing of the extraction was determined after examining the results of 168 analyses of Lake Malawi sediments using a more labor intensive, time-series procedure (24).

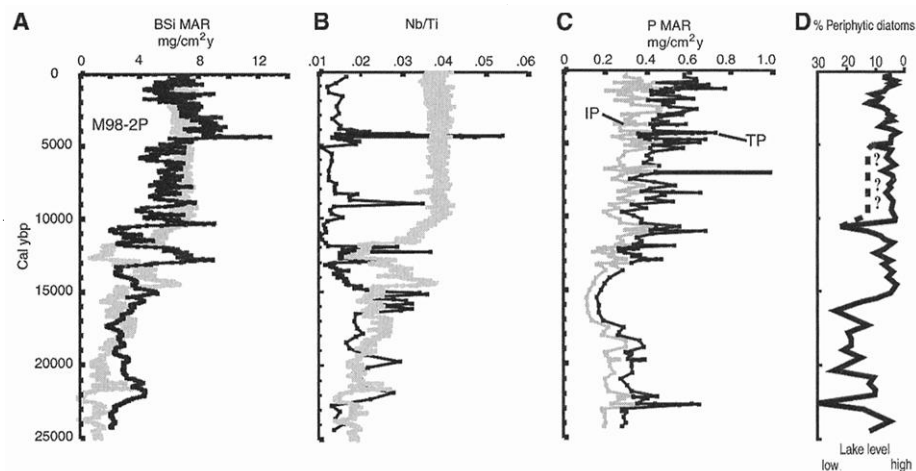


**Fig. 3.** Geochemical and paleontological data from Malawi compared to data from the Greenland record. (A) Comparison of smoothed (five-point running average) profiles of BSi MAR (indicated by the black line) in core M98-2P and the GRIP record of δ<sup>18</sup>O (indicated by the gray line). (B) Comparison of the ratio of Nb/Ti (indicated by the black line) in core M98-2P and GRIP δ<sup>18</sup>O (indicated by the gray line). Nb/Ti ratios were determined by inductively coupled plasma-mass spectrometry on total sediment digests. Repeated analyses of reference material [from the National Institute of Standards and Technology (NIST) and the Geological Survey of Canada (GSC)] suggest precision and accuracy for this ratio of <4%. (C) Inorganic phosphorus (indicated by the gray line) and TP (indicated by the black line) MARs in M98-2P. Phosphorus was analyzed in the sediments after the procedure in (25). Recoveries on NIST reference materials are >94% for total P, and the precision is <5%. (D) Percent abundance of periphytic (benthic) diatoms in M98-2P. Benthic diatoms live in the photic zone (i.e., in a water depth shallower than 100 m). Their high abundance in this core from a 363-m depth suggests that the lake level was substantially lower than it is at present. The scale of benthic diatom abundance has been reversed. The dashed line on the water level curve between 10 and 5 ka indicates a lake level somewhat lower than the benthic diatom record implies, based on endogenic carbonates found in cores of this age from the south basin (23).

## REPORTS

rived from these volcanoes are observed in the piston cores and date at 4.4 and 9.1 ka. Discounting the sharp peaks associated with these layers, the Nb/Ti ratio appears to have higher average values in the Pleistocene than in the Holocene sediments (Fig. 3). North winds blowing over the cool, dry volcanic landscape would have transported ash to the lake, resulting in a higher Nb/Ti ratio in lake sediments (13). Such winds, which would have caused upwelling and increased diatom productivity at the north end of the lake, may be a regional response to global shifts in the late Pleistocene climate. For example, a more southward excursion of the Intertropical Convergence Zone (ITCZ) during austral summer would expose northern Malawi and southwestern Tanzania to the northeasterly winds of the northern side of the ITCZ.

The first dramatic shift in the diatom production of northern Lake Malawi to Holocene-like conditions started at 13 ka, perhaps slightly ahead of, or coincidentally with, the onset of the Younger Dryas in the Northern Hemisphere. The benthic diatom record suggests that the lake level had already risen substantially, more than 2000 years previously. The region's climate was moister than it was during the Pleistocene, and the biology in the north basin was poised to respond. We hypothesize that this biological response was triggered by the onset of north winds associated with the Younger Dryas, and perhaps by the termination of the Antarctic Cold Reversal, which marked the resumption of warming to Holocene conditions in the high southern latitudes.

Diatom productivity may not reflect primary production as a whole. It is conceivable that primary productivity by some other group of phytoplankton, such as green or blue-green al-

gae, had already increased by 15.7 ka, when the periphytic diatom record indicates that the lake level rose. However, the total phosphorus (TP) MAR resembles the BSi MAR in M98-2P, at least on a glacial to interglacial scale (Fig. 3). The TP MAR profile does not show nearly as much structure as does the BSi MAR, and in particular does not show the pronounced two-step transition from glacial to interglacial conditions (14). Nevertheless, the rise in the TP MAR to Holocene values accompanies the more abrupt rise in the BSi MAR at 13 ka, not when the lake level rose at 15.7 ka.

The inverse correlation between the Malawi BSi MAR and GRIP records breaks down after 11 ka, after which time the Malawi record exhibits considerable change in the Holocene, whereas the GRIP record remains remarkably stable. The climatic tie to the high latitudes of the north appears to have weakened considerably with the demise of the continental ice sheets.

Nevertheless, subtle century-scale links remain between the climate of the Northern Hemisphere and the Lake Malawi basin. The BSi MAR in northern Lake Malawi was elevated during the Little Ice Age (15). This relation of elevated BSi MAR during the cool times of the Northern Hemisphere's Little Ice Age is consistent with the Pleistocene trends presented in this study. It is also compatible with the observed low BSi MAR at 1 ka, the time of the Medieval Warm Period in the Northern Hemisphere.

The BSi MAR was relatively low around 9.5 ka, 5.8 ka, and 1 ka, and it was higher than average from 4.3 to 2 ka (Fig. 3). Periods of exceptional aridity in North Africa, attributed to weak monsoons, occurred around 12.4, 8.2, 6.6, and 4.0 ka (1). The three most

arid of these periods (12.4, 8.2, and 4.0 ka) coincided with times of relatively high diatom productivity in northern Lake Malawi. This may reflect an inverse relation in rainfall between the Malawi basin and regions to the north (16). Alternatively it may indicate that arid times in North Africa occur when the ITCZ remains longer at its southern terminus during austral summer, promoting more frequent north winds over the Malawi basin.

The climate of Africa is complex due to the continent's size and heterogeneous landscape. Although teleconnections in rainfall anomaly patterns have been identified within the continent [e.g., (17)], their links to the global climate system remain elusive and beyond the predictive capabilities of the present generation of general circulation models (18). Nevertheless, our results suggest a tie between cold conditions in the Northern Hemisphere and north winds over the northern Malawi basin, perhaps in response to a more southward excursion of the ITCZ under such circumstances. These results provide the first high-resolution record of climate variability in the southern African tropics that extends back to the LGM.

### References and Notes

1. F. Gasse, *Quat. Sci. Rev.* **19**, 189 (2000).
2. D. A. Livingstone, in *Biological Relationships Between Africa and South America*, P. Goldblatt, Ed. (Yale University Press, New Haven, 1993), pp. 455–472.
3. All six piston cores were analyzed for magnetic susceptibility using a Geotek Multi-Sensor Core Logger (Northamptonshire, UK). Water content and total organic carbon were determined at 10-cm intervals down each core, by weight loss after drying and coulometry, respectively. Stratigraphic correlations were established among the cores and were based on sedimentary structures, magnetic susceptibility, and percent abundance of BSi: The cores contain an upper varved interval that averages about a meter in thickness, overlying an interval that is about 2.5-m thick, consisting of alternating packets of varved and non-varved sediments. The varves in both intervals are about 0.5- to 0.7-mm thick, and the packets are typically about 2- to 8-cm thick. These overlie another continuously varved interval that spans about 1.2 to 2 m, which, in turn, overlies a second interval of alternating packets of varves and nonvarved sediment of about a meter thickness. The bottom unit in the cores is a homogenous silty clay, up to 3-m thick.
4. H. A. Bootsma, R. E. Hecky, *Water Quality Report: Draft Document* [South African Development Community/Global Environmental Facility (SADC/GEF), Lake Malawi Nyasa Biodiversity Conservation Project, 1998].
5. G. Patterson, O. Kachinjika, in *The Fishery Potential and Productivity of the Pelagic Zone of Lake Malawi/Niassa*, A. Menz, Ed. (Natural Resources Institute, Overseas Development Administration, Chatham, UK 1995), pp. 1–68.
6. L. Vidal et al., *Clim. Dyn.* **15**, 909 (1999).
7. T. C. Johnson, in *Sedimentation in Continental Rifts*, R. W. Renaut, G. M. Ashley, Eds. (Society of Economic Paleontologists and Mineralogists, Tulsa, OK, in press).
8. F. Gasse, P. Barker, T. C. Johnson, in *The East African Great Lakes: Limnology, Palaeoclimatology and Biodiversity*, E. O. Odada, D. O. Olago, Eds. (Kluwer Academic Publishers, Dordrecht, Netherlands, in press).
9. T. C. Johnson, P. Ng'ang'a, in *Lacustrine Basin Exploration: Case Studies and Modern Analogs*, B. J. Katz, Ed. (American Association of Petroleum Geologists, Tulsa, OK, 1990), pp. 113–136.
10. S. L. Barry, thesis, University of Minnesota (2001).
11. The possibility that the Nb/Ti versus BSi relation is an artifact of the BSi analytical technique for extracting Si

**Table 1.** Radiocarbon dates from cores M98-1P and M98-2P. Dates beginning with "AA" were determined at the University of Arizona, and dates beginning with "NOSAMS" were determined at the Woods Hole Oceanographic Institution. Bulk organic carbon was dated in some samples; in others, pollen extracts (the organic residue from standard pollen preparation procedures) were dated. There was no substantial difference between dates of these different components when compared on replicate samples (10). The ages were corrected by subtracting 450 years from the reported radiocarbon age, based on core-top dates in a multicore from the north basin immediately adjacent to core site M98-1P (10). The corrected radiocarbon dates were converted to calendar age using the program, CALIB version 4.3 for Macintosh, provided by the University of Washington (26).

Core	Lab #	Depth in cm	C <sup>14</sup> age	SD	Calendar age
M98-1P	AA32943	55	1880	55	1358
	AA32944	166	4015	60	3888
	AA32945	306.5	6270	65	6700
	AA32946	460.5	9010	85	9582
	AA32947	627.5	13330	100	15561
	AA32948	765.5	19010	270	22086
M98-2P	NOSAMS 20475	139.5	2510	50	2048
	NOSAMS 20476	248.5	4020	65	3893
	NOSAMS 20477	379	6260	65	6688
	NOSAMS 20480	500.5	8820	110	9477
	NOSAMS 20478	537.5	9550	120	10248
	NOSAMS 19968	648.5	11450	100	13048
	NOSAMS 20485	744	15150	130	17644
	NOSAMS 20481	900	21000	240	24333

# Asteroid 1950 DA's Encounter with Earth in 2880: Physical Limits of Collision Probability Prediction

J. D. Giorgini,<sup>1</sup> \* S. J. Ostro,<sup>1</sup> L. A. M. Benner,<sup>1</sup> P. W. Chodas,<sup>1</sup> S. R. Chesley,<sup>1</sup> R. S. Hudson,<sup>2</sup> M. C. Nolan,<sup>3</sup> A. R. Klemola,<sup>4</sup> E. M. Standish,<sup>1</sup> R. F. Jurgens,<sup>1</sup> R. Rose,<sup>1</sup> A. B. Chamberlin,<sup>1</sup> D. K. Yeomans,<sup>1</sup> J.-L. Margot<sup>5</sup>

Integration of the orbit of asteroid (29075) 1950 DA, which is based on radar and optical measurements spanning 51 years, reveals a 20-minute interval in March 2880 when there could be a nonnegligible probability of the 1-kilometer object colliding with Earth. Trajectory knowledge remains accurate until then because of extensive astrometric data, an inclined orbit geometry that reduces in-plane perturbations, and an orbit uncertainty space modulated by gravitational resonance. The approach distance uncertainty in 2880 is determined primarily by uncertainty in the accelerations arising from thermal re-radiation of solar energy absorbed by the asteroid. Those accelerations depend on the spin axis, composition, and surface properties of the asteroid, so that refining the collision probability may require direct inspection by a spacecraft.

Useful predictions of asteroid encounters with planets, in which the statistical uncertainty in the time of closest approach is  $\pm 10$  days or less, are generally limited to an interval within a few decades of the time spanned by positional measurements (astrometry), unless optical astrometry spans several years or high-precision delay-Doppler radar measurements are available. This is because long-term solar system dynamics can be a highly nonlinear prediction problem, and measurement error propagation increases the positional uncertainties of an asteroid with time. Here we consider the trajectory of asteroid 1950 DA over a much longer time period and estimate the probability of an Earth encounter.

The possibility of a close approach to Earth was initially recognized in the course of a recent radar experiment that used dynamical force propagation methods that have been used successfully for previous, comparatively short-term predictions of asteroid orbits. Then, because of the quality and extent of the orbit measurements, we examined several factors that are normally neglected in asteroid trajectory prediction and hazard studies so as to more accurately characterize trajectory

knowledge and confirm the initial impact probability calculation. These factors include computational noise, galactic tides, perturbations due to the gravitational encounters of the asteroid with thousands of other asteroids, an oblate Sun whose mass is decreasing, the role of planetary mass uncertainties, acceleration due to solar wind and radiation pressure acting on the asteroid, and the acceleration of the asteroid due to thermal emission of absorbed solar energy.

Asteroid (29075) 1950 DA was discovered on 23 February 1950 (1). It was observed for 17 days and then lost until an object discovered on 31 December 2000 and designated 2000 YK66 (2) was recognized just 2 hours later as being the long-lost 1950 DA (3). We conducted delay-Doppler radar observations using methods described by Ostro (4) at Goldstone and Arecibo on 3 to 7 March 2001, during the asteroid's  $7.79 \times 10^6$  km approach to Earth (a distance 20.3 times larger than that separating Earth and the Moon). Our echoes (Fig. 1) reveal a slightly asymmetrical spheroid with a mean diameter of 1.1 km.

Our first radar observations, at Goldstone, corrected the initial orbit prediction by  $-35 \pm 35$  mm s<sup>-1</sup> in radial velocity and  $+7.9 \pm 0.9$  km in range (5). We incorporated this radar astrometry in a weighted least-squares orbit estimation for a 10 March 2001 epoch (6). Then, to determine the time interval over which approaches to planetary bodies could be accurately predicted, we mapped the known orbit uncertainties at the solution epoch (contained in the measurement covariance matrix) to other times by numerically integrating the equations

from weathered ash is precluded by a strong inverse relation ( $r^2 = 0.63$ ,  $n = 184$ ) between BSi and Ti (i.e., BSi dilutes Ti-bearing aluminosilicates). Furthermore, microscopic examination of the sediments reveals an abundance of diatoms and only an occasional volcanic glass shard, except in the two distinct tephra layers. The Nb-enriched volcanoclastic debris, in fact, is primarily weathered residue of volcanic ash, not unweathered glass shards. The observed variability in BSi is thus not a result of enhanced preservation brought on by the presence of volcanic ash.

12. D. A. Harkin, *Tanagnyika Notes* **40**, 20 (1955).
13. The volcanoclastic material also could have been transported to the lake basin by rivers. However, this mechanism is not consistent with the fact that the lake level was low (i.e., the climate was relatively dry) during the time of high Nb/Ti ratio in the sediments. Also, there are no major ash layers in the Pleistocene sections of these cores, whereas there are two in the Holocene sections where, on average, the Nb/Ti ratio in the sediments is lower than that in the Pleistocene. In addition, water transport of volcanoclastic material to the northern basin would not necessarily result in higher diatom burial there. Silica is recycled through several generations of diatoms in a large lake before it is buried in the underlying sediment (7, 19) and in the process will be well mixed throughout the entire lake. A point source of dissolved silica in the north basin would not affect diatom production and burial there as effectively as would upwelling associated with north winds.
14. Differences between the biogenic silica and phosphorus records are not surprising. Changes in soil development associated with varying climate or volcanic sources of P and BSi will influence the nutrient source function to the lake (20, 21). Furthermore, the lake's internal phosphorus cycle is likely to be tightly coupled to the redox behavior of iron, especially where the chemocline, marking the boundary between oxic and anoxic waters, intersects the lake floor. The chemocline is presently at about a 200-m depth in Lake Malawi, but it has migrated vertically by more than 100 m during the Holocene (22, 23). This dynamic behavior of the chemocline very likely affects the geochemical mass balance of phosphorus in Lake Malawi in ways that will affect its delivery to sediments in the deep, anoxic basins offshore.
15. T. C. Johnson, S. L. Barry, Y. Chan, P. Wilkinson, *Geology* **29**, 83 (2001).
16. S. A. Nicholson, in *Environmental Change and Response in East African Lakes*, J. T. Lehman, Ed. (Kluwer Academic, Dordrecht, Netherlands, 1998), pp. 207–232.
17. S. E. Nicholson, in *The Limnology, Climatology, and Paleoclimatology of the East African Lakes*, T. C. Johnson, E. O. Odada, Eds. (Gordon and Breach, Toronto, 1996), pp. 25–56.
18. Climate Variability and Predictability (CLIVAR) Project, *Climate Research for Africa: WCRP No. 16/1999* (World Climate Research Program, 1999).
19. T. C. Johnson, S. J. Eisenreich, *Geochim. Cosmochim. Acta* **43**, 77 (1979).
20. O. A. Chadwick, L. A. Derry, P. M. Vitousek, B. J. Huebert, L. O. Hedin, *Nature* **397**, 491 (1999).
21. G. M. Filipelli, C. Souch, *Geology* **27**, 171 (1999).
22. E. T. Brown, L. Le Gallonnet, C. R. German, *Geochim. Cosmochim. Acta* **64**, 3515 (2000).
23. B. P. Finney, T. C. Johnson, *Palaeogeogr. Palaeoclimatol. Palaeoecol.* **85**, 351 (1991).
24. D. J. DeMaster, thesis, Yale University (1979).
25. K. I. Aspila, H. Aegemian, A. S. Y. Chau, *Analyst* **101**, 187 (1976).
26. M. Stuiver, P. J. Reimer, *Radiocarbon* **35**, 215 (1993).
27. We thank the government of Malawi for access to Lake Malawi and logistical support for our work in the field; the SADC/GEF Lake Malawi/Nyasa Biodiversity Conservation Project at Senga Bay for housing, laboratory facilities, and ship time aboard the R/V *Usipa*, under the able command of M. Day; M. Talbot for comments on an earlier draft of this manuscript and, along with M. Fillipi, for assistance in the field. Y. Chan, S. Grosshuesch, and J. Agnich contributed substantially in the laboratory. This material is based on work supported by the NSF under grant no. ATM-9709291. This is publication no. 131 of IDEAL.

22 January 2002; accepted 20 February 2002

<sup>1</sup>Jet Propulsion Laboratory, California Institute of Technology, Pasadena, CA 91109–8099, USA.

<sup>2</sup>School of Electrical Engineering and Computer Science, Washington State University, Pullman, WA 99164–2752, USA. <sup>3</sup>Arecibo Observatory, Arecibo, Puerto Rico 00612, USA. <sup>4</sup>Lick Observatory, University of California, Santa Cruz, CA 95064, USA. <sup>5</sup>California Institute of Technology, Pasadena, CA 91125, USA.

\*To whom correspondence should be addressed. E-mail: Jon.Giorgini@jpl.nasa.gov